GIScience & Remote Sensing
Publication details, including instructions for authors and subscription information:
http://www.tandfonline.com/loi/tgrs20

Mapping impervious surface area in the Brazilian Amazon using Landsat Imagery

Guiying Li [a], Dengsheng Lu [b], Emilio Moran [b] & Scott Hetrick [a]
[a] Anthropological Center for Training and Research on Global Environmental Change (ACT), Indiana University, Student Building 331, 701 E. Kirkwood Ave, Bloomington, IN, 47405, USA
[b] Center for Global Change and Earth Observations, Michigan State University, 1405 S. Harrison Road, East Lansing, MI, 48823, USA
Published online: 14 Jun 2013.

To cite this article: Guiying Li, Dengsheng Lu, Emilio Moran & Scott Hetrick (2013): Mapping impervious surface area in the Brazilian Amazon using Landsat Imagery, GIScience & Remote Sensing, DOI:10.1080/15481603.2013.780452

To link to this article: http://dx.doi.org/10.1080/15481603.2013.780452

GIScience & Remote Sensing, 2013
http://dx.doi.org/10.1080/15481603.2013.780452

Taylor & Francis
Taylor & Francis Group

Mapping impervious surface area in the Brazilian Amazon using Landsat Imagery

Guiying Li[a], Dengsheng Lu[b]*, Emilio Moran[b] and Scott Hetrick[a]

[a]*Anthropological Center for Training and Research on Global Environmental Change (ACT), Indiana University, Student Building 331, 701 E. Kirkwood Ave., Bloomington, IN 47405, USA;* [b]*Center for Global Change and Earth Observations, Michigan State University, 1405 S. Harrison Road, East Lansing, MI 48823, USA*

(*Received 12 September 2012; final version received 21 February 2013*)

Impervious surface area (ISA) is an important parameter related to environmental change and socioeconomic conditions, and has been given increasing attention in the past two decades. However, mapping ISA using remote sensing data is still a challenge due to the variety and complexity of materials comprising ISA and the limitations of remote sensing data spectral and spatial resolution. This paper examines ISA mapping with Landsat Thematic Mapper (TM) images in urban and urban–rural landscapes in the Brazilian Amazon. A fractional-based method and a per-pixel based method were used to map ISA distribution, and their results were evaluated with QuickBird images based on the 2010 Brazilian census at the sector scale of analysis for examining the mapping performance. This research showed that the fraction-based method improved the ISA estimation, especially in urban–rural frontiers and in a landscape with a small urban extent. Large errors were mainly located at the sites having ISA proportions of 0.2–0.4 in a census sector. Calibration with high spatial resolution data is valuable for improving Landsat-based ISA estimates.

Keywords: impervious surface area; Landsat; spectral mixture analysis; urban–rural landscape

1. Introduction

Impervious surface area (ISA) is defined as any man-made land surface that water cannot infiltrate. It is an important parameter in environmental, demographic, and socioeconomic related research (Schueler 1994; Arnold and Gibbons 1996; Zug et al. 1999; Brabec, Schulte, and Richards 2002; Lu et al. 2010; Myint et al. 2010). Therefore, mapping of ISA has seen increased attention in the past two decades (Slonecker, Jennings, and Garofalo 2001; Brabec, Schulte, and Richards 2002; Slonecker and Tilley 2004; Weng 2007; Tullis et al. 2010; Weng 2012). ISA has often been mapped using per-pixel based classification methods, such as maximum likelihood (Goetz et al. 2003; Lu et al. 2012). Because of the complexity of urban landscapes, the diversity of construction materials, and the constraints of remotely sensed data, classification-based ISA results are often poor, especially for area estimates in urban–rural landscapes (Lu, Moran, and Hetrick 2011). Thus, the monitoring of urban expansion and area estimation of urbanization generated high uncertainty (Lu, Moran, and Hetrick 2011). Since Ridd (1995) proposed the V–I–S (vegetation–impervious surface–soil) model, much progress has been made to improve

*Corresponding author. Email: ludengsh@msu.edu

ISA mapping performance using spectral decomposition methods (Wu and Murray 2003; Wu 2004; Lu and Weng 2006).

Many methods and techniques for mapping ISA distribution with satellite images have been summarized in the literature (e.g., Lu and Weng 2006; Lu et al. 2012; Weng 2012). Previous studies on mapping ISA mainly concentrated on large cities (Wu 2004; Lu and Weng 2006) because of their importance. However, urban expansion often occurs in urban–rural frontiers (Lu, Moran, and Hetrick 2011). It is necessary to accurately map ISA distribution and monitor its dynamic change in the urban–rural frontiers, but how to effectively estimate the ISA in such a complex landscape has not been fully examined. Therefore, the objective of this research was to examine how different urban landscapes with various urban extents and patterns in the Brazilian Amazon affected ISA mapping performance.

2. Overview of ISA mapping with linear spectral mixture analysis

Although many methods have been developed for mapping ISA (Lu et al. 2012; Weng 2012), the linear spectral mixture analysis (LSMA) has been regarded as the most appropriate method (Wu 2004; Lu and Weng 2006; Lu, Moran, and Hetrick 2011; Weng 2012). One critical step using the LSMA is to select good-quality endmembers (pure materials). Different image transform methods such as minimum noise fraction (MNF) transform are often used to convert the original Landsat multispectral data into a new dataset so that major information is concentrated in just the first three components (Lu and Weng 2006). The endmembers are then identified from the scatterplots of the first three MNF components, assuming that endmembers are located at the vertices of the scatterplots (Lu and Weng 2004). In an urban landscape, four endmembers – high-albedo object, low-albedo object, green vegetation, and soil are often used and they can be identified from the scatterplots of MNF components (Lu and Weng 2004). A constrained least-squares solution is then used to unmix the Landsat multispectral image into four fractional images. Much previous literature has detailed the LSMA approach (Wu and Murray 2003; Lu and Weng 2004), thus, this paper will not provide a detailed description.

As previous research has indicated that ISA is mainly concentrated in the high-albedo and low-albedo fraction images (Wu and Murray 2003; Lu and Weng 2006; Lu, Moran, and Hetrick 2011), ISA can be viewed as a linear combination of high-albedo and low-albedo objects. Bright ISA and some bare soils are often concentrated in the high-albedo fraction image, and dark ISA, water/wetland, and shadows are often concentrated in low-albedo fraction images. One critical step in extracting ISA is to remove the non-ISA components in the high-albedo and low-albedo fraction images. Lu and his colleagues have explored different methods, such as the integration of land surface temperature and unsupervised classification, to remove the non-ISA pixels (Lu and Weng 2006; Lu, Moran, and Hetrick 2011).

3. Methods

The cities of Santarém in Pará State and Lucas do Rio Verde (hereafter referred to as Lucas) in Mato Grosso State, Brazil, were selected for this study (Figure 1). The Santarém study area is located at the confluence of the Tapajós and the Amazon rivers. The area was the site of one of the three most important prehistoric populations studied to date in the Amazon. The city of Santarém was officially founded by Jesuit priests over 300 years ago and is now an important port city. Lucas is connected to Santarém and to the heart of

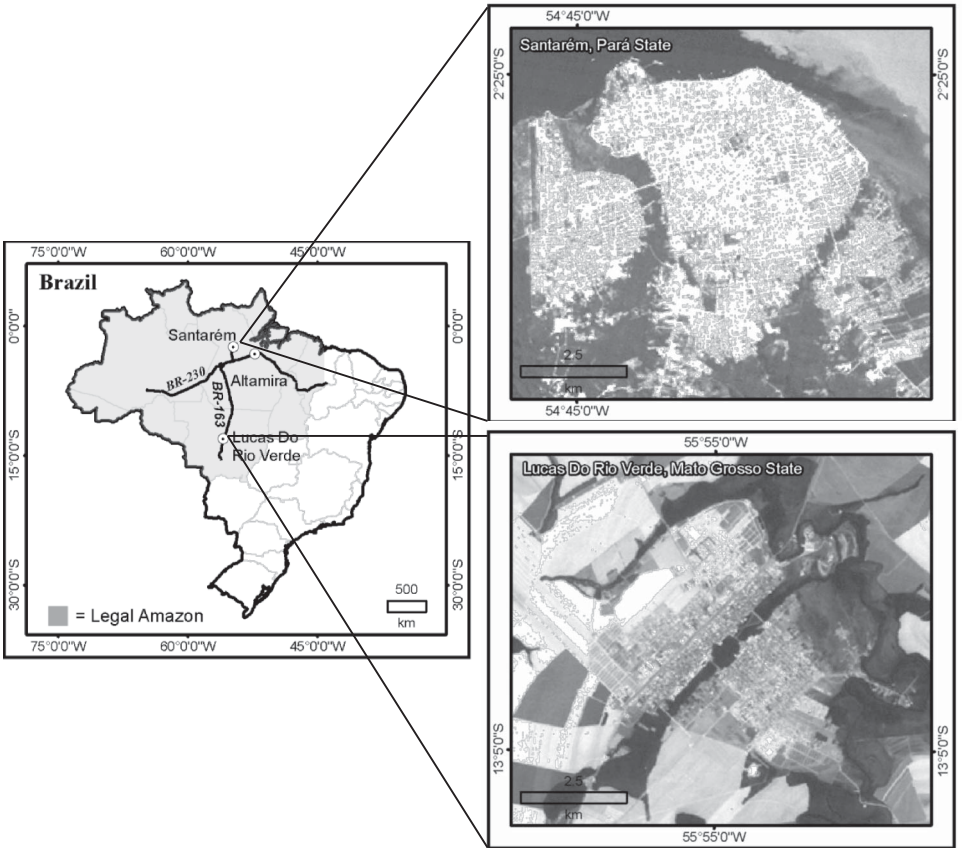

Figure 1. Study areas – Santarém in Pará State and Lucas do Rio Verde in Mato Grosso State.

Brazil's soybean-growing region at Cuiabá via the BR-163 highway, which runs through Lucas. This settlement growth accompanied the beginnings of soy expansion in Mato Grosso as a whole and led to the establishment of Lucas County (the area had been part of two other counties) in 1982. Lucas has a relatively short history and small urban extent but has experienced rapid urbanization. According to the 2010 census data, population in Santarém city was 204,129 and in Lucas city was 42,068 (http://www.ibge.gov.br/cidadesat/topwindow.htm?1).

The framework for mapping ISA from Landsat Thematic Mapper (TM) images is illustrated in Figure 2. The major steps include (1) developing four fraction images from a TM multispectral image using LSMA approach, (2) developing initial dark and bright ISA images using thresholds on low-albedo and high-albedo fraction images, respectively, (3) extracting a TM spectral image for both initial dark and bright ISA pixels and conducting an unsupervised classification, respectively, (4) generating a per-pixel based ISA image by combining dark and bright ISA images, (5) generating a fraction ISA image by combining the per-pixel based ISA image and the sum of high-albedo and low-albedo fraction images, and (6) evaluating and comparing the per-pixel and fraction ISA images with the QuickBird-derived ISA image.

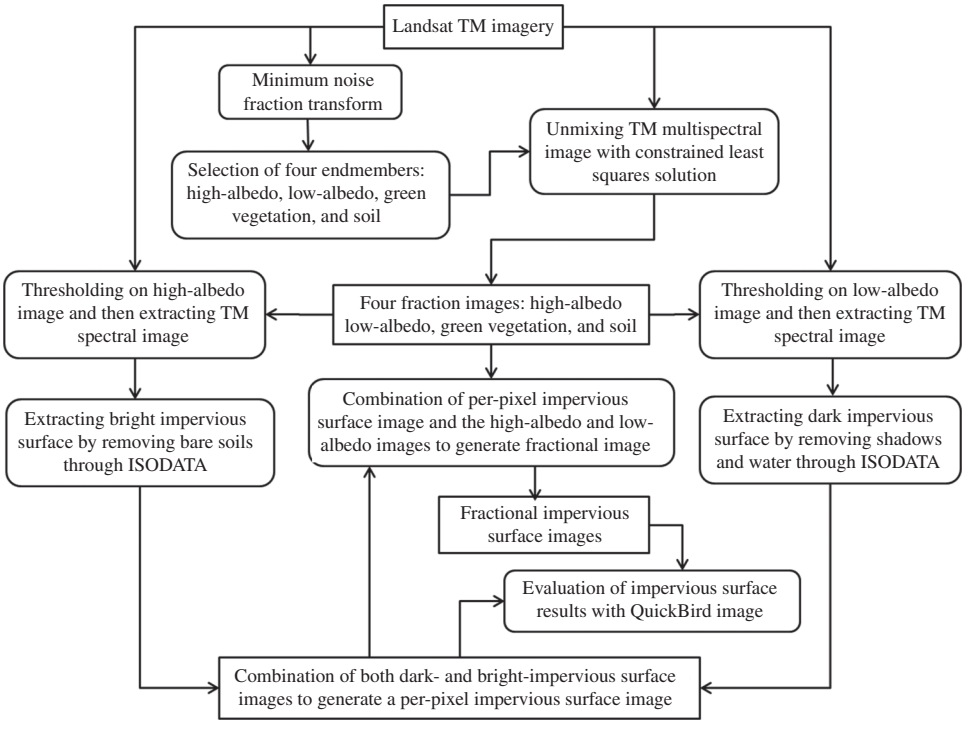

Figure 2. Strategy of mapping impervious surface distribution with Landsat TM images.

3.1. *Image collection and preprocessing*

A Landsat 5 TM image (path/row: P227/R062) acquired on 29 June 2010 and a QuickBird image acquired on 25 June 2008 for Santarém, and a Landsat 5 TM image (path/row: P227/R069) acquired on 22 May 2008 and a QuickBird image acquired on 20 June 2008 for Lucas were used in this research. Both TM images with spatial resolution of 30 m were geometrically rectified into Universal Transverse Mercator (UTM) coordinate system (UTM zone 21 for both study areas) with root mean square errors (RMSEs) of <0.5 pixels. Radiometric and atmospheric calibration for both TM images was implemented with the dark-object subtraction method (Chavez 1996; Chander, Markham, and Helder 2009) and the results were re-scaled to 8-bit data format (i.e., data range between 0 and 255). The QuickBird-derived ISA data were used for evaluation of the TM-derived ISA estimates based on the 2010 Brazilian census sector polygons.

3.2. *Development of impervious surface data with Landsat images*

In this research, four endmembers – high-albedo object, low-albedo object, green vegetation, and soil – were identified from three MNF components, which were transformed from the Landsat TM multispectral image (Lu and Weng 2006). Four fraction images were then developed from the TM multispectral image using the constrained least-squares solution. In order to remove the non-ISA pixels in the high-albedo and low-albedo fraction images, thresholds were selected separately from the high-albedo and low-albedo fraction images based on the comparison of these fraction images and the QuickBird-

derived ISA images. The TM spectral signatures for bright and dark ISA pixels were extracted and then classified into 60 clusters using cluster analysis (i.e., ISODATA). The analyst examined each cluster to determine whether the cluster was ISA or not so that non-ISA pixels were removed.

After non-ISA pixels were removed from the dark- and bright-ISA images, both images were combined to generate a per-pixel based ISA image. Meanwhile, the fractional ISA image was extracted from the sum of the high-albedo and low-albedo fraction images by masking non-ISA pixels out from the per-pixel ISA image. In this way, two products of ISA images – pixel-based and fraction-based ISA images were extracted.

3.3. *Evaluation of impervious surface images with QuickBird images*

Both per-pixel and fractional ISA products were evaluated with the reference data developed from QuickBird images for both study areas. Our previous research has indicated that the hybrid method can successfully extract ISA data from very high spatial resolution satellite images such as QuickBird (Lu, Hetrick, and Moran 2011). The hybrid method is based on the combined use of a thresholding technique, cluster analysis, and manual editing. This method is detailed in Lu, Hetrick, and Moran (2011) and the major steps are summarized as following: (1) producing the normalized difference vegetation index (NDVI) image from QuickBird red and near-infrared (NIR) bands and then mask vegetation out with the selected threshold on the NDVI image; and mask water bodies out with the threshold on the NIR band; (2) extracting spectral signatures of the non-vegetation pixels, and using cluster analysis to classify the extracted spectral signatures into 50 clusters. The analyst was responsible for merging the clusters into ISA and other land cover classes; (3) manually editing the extracted ISA image to eliminate the non-ISA such as bare soils, shadows, and wetlands which were included in the ISA class due to spectral confusion. In order to make sure the derived ISA data had sufficiently high accuracy, a total of 400 test samples were selected with the random sampling method in Santarém and 450 test samples for Lucas due to its relatively small proportion of urban areas. The analyst examined each test sample plot to decide whether it was correctly classified as ISA or not (Lu, Hetrick, and Moran 2011).

The evaluation of Landsat-derived ISA results was conducted based on the 2010 census sector scale of analysis. All the ISA data from Landsat TM images and from QuickBird image for both study areas were calculated for each census sector based on per-pixel and fractional ISA images. Five ISA categories – very low, low, medium, high, and very high were grouped based on reference data ranges: less than 0.2, [0.2–0.4], [0.4–0.6], [0.6–0.8] and greater than 0.8 (Note: [0.2–0.4] means the data range of greater than or equal to 0.2 but less than 0.4). In addition to the analysis of overall errors, residue and RMSE at census sector scale for each ISA category was also conducted, and expressed as

$$\textit{Residue for } x_i = x_{ei} - x_{ri} \tag{1}$$

$$\text{RMSE} = \sqrt{\frac{\sum_{i=1}^{n}(x_{ei} - x_{ri})^2}{n}} \tag{2}$$

where x_{ei} and x_{ri} are estimates and reference values for sector i and n is the number of sectors in a study area. A scatterplot consisting of ISA estimates and reference data was used to examine their relationship and to analyze the potential solution to calibrate the estimates.

4. Results and discussion

4.1. Analysis of fraction images

Development of high-quality fraction images is critical for generating accurate ISA data. The four fraction images which were developed from Landsat TM multispectral images using LSMA are illustrated in Figure 3, indicating that ISA is mainly concentrated on the high-albedo and low-albedo fraction images. In the high-albedo fraction image, bright ISA and some bare soils (especially in Lucas) are highlighted (see Figure 3a and 3e), while the low-albedo fraction image highlights dark ISA (mainly roads in Santarém) and water bodies (see Figure 3b and 3f). This figure also indicates a large proportion of dark ISA, especially roads in Santarém, but limited areas in Lucas. This situation is related to different construction materials in an urban landscape. As shown in Figure 4, the impervious surface materials appearing as white and light yellow in the color composites (Figure 4) have high spectral signatures in the TM multispectral image, thus, they mainly reflect high fraction values in the high-albedo fraction image (Figure 3a and 3e). Large amounts of impervious surface materials in Santarém have dark gray (e.g., roads) and dark brown colors (e.g., building roofs) (see Figure 4a) and they have low spectral signatures, thus these ISA pixels are mainly distributed in the low-albedo fraction image (Figure 3b). In contrast, Lucas has impervious surface materials in cyan/aquamarine or white color on the color composite (Figure 4b), thus, these impervious surfaces have relatively high spectral signatures, and they are mainly reflected in the high-albedo fraction image, and very limited areas are in the low-albedo fraction image (Figure 3f). Figure 3 also illustrates that no ISA is found in the green vegetation fraction image because ISA has significantly different spectral characteristics than vegetative cover. However, some dirty roads in rural regions appear in the soil fraction image because of their similar spectral features with bare soils. This is one source of uncertainty of ISA estimation in rural regions.

4.2. Analysis of impervious surface results

The reference data for evaluating Landsat-derived ISA estimates were developed from the QuickBird images using the hybrid method, as illustrated in Figure 5. Based on analysis of test samples, overall accuracies of 98.7% for Santarém and of 98.2% for Lucas were obtained. Therefore, the QuickBird-derived ISA data provided sufficiently accurate reference data for evaluating the TM-derived ISA results. Figure 5 indicates that Santarém city is a developed urban landscape with large urban extents, but Lucas is a developing urban landscape with much smaller urban extents and a large proportion of roads in urban–rural frontiers.

The fractional ISA images in the Santarém and Lucas study areas (see Figure 6) indicate that a large proportion of the Santarém study area has high fractional values, and conversely, a large proportion of Lucas study area has low fractional values, implying that different urban landscapes affect ISA distribution patterns. Santarém has a long history of city development with a relatively large urban extent and dense urban ISA, while Lucas has a short history with a relatively small urban extent and relatively sparse urban ISA distribution. Santarém has obvious ISA change trends, from highest fraction values in the urban landscape to gradually decreasing fraction values in urban–rural frontiers in the southeast and western parts of the city. In Lucas, only a small area in the northern part of the city has relatively high fraction values.

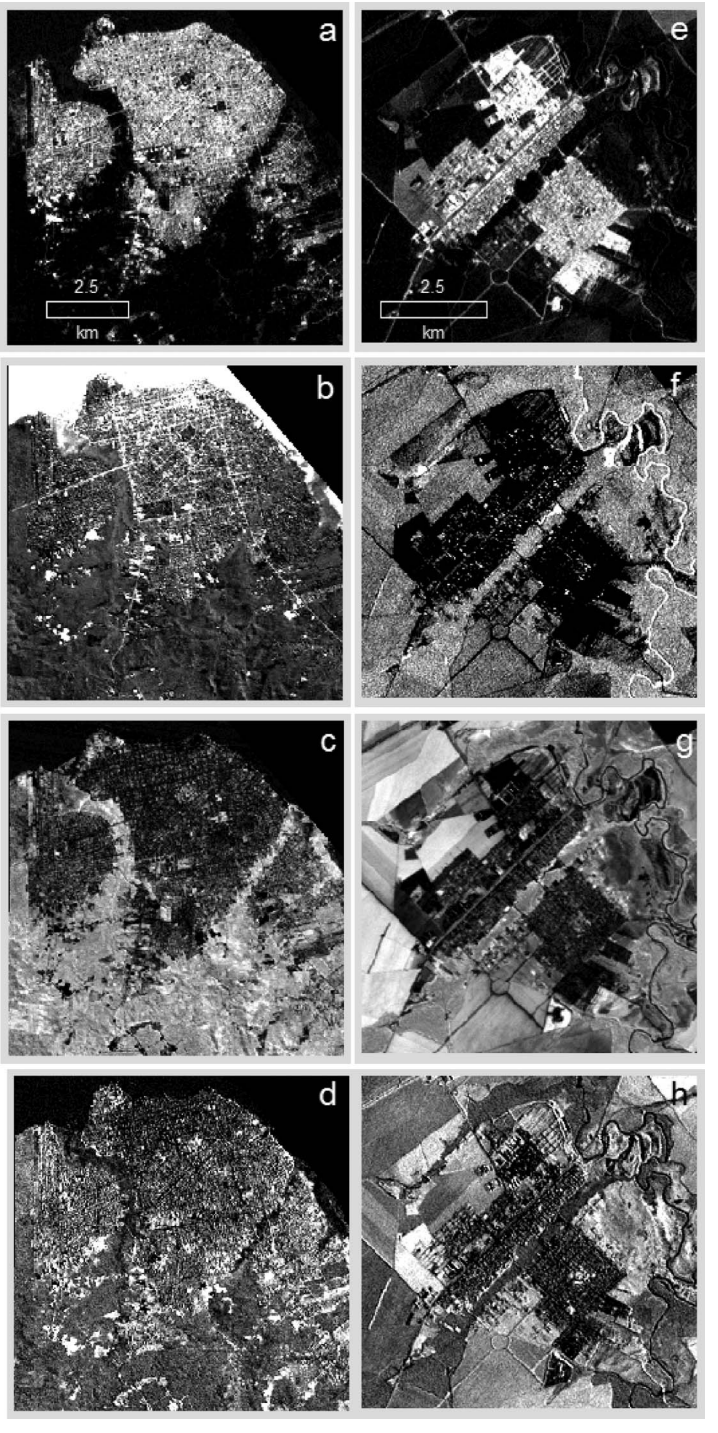

Figure 3. Four fraction images – high albedo, low-albedo, green vegetation, and soil in Santarém – a, b, c, d and in Lucas – e, f, g, h, which were developed from Landsat TM images with the spectral mixture analysis approach.

Figure 4. False-color composites from QuickBird images showing the complexity of impervious surface distribution in Santarém and Lucas.

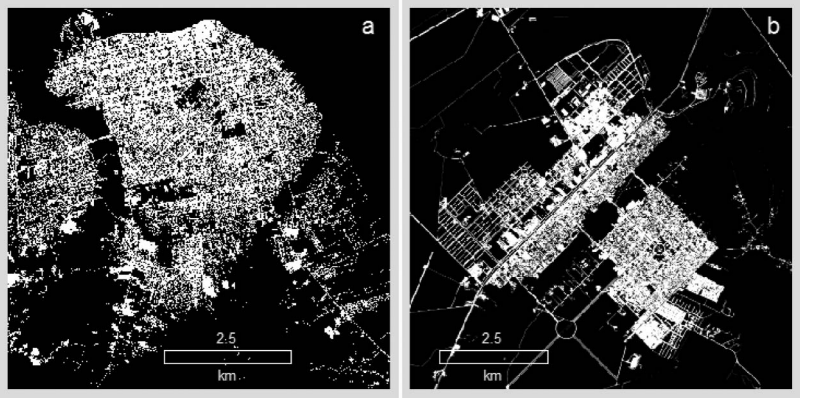

Figure 5. Impervious surface images in Santarém (a) and Lucas (b), which were developed from QuickBird images.

Analysis of residuals indicated that the per-pixel based results overestimated considerably ISA in both study areas and the fraction-based method considerably reduced this problem, especially in Lucas (see Figure 7). Overall, the residuals reached a peak when ISA in a sector was around 0.4 in Santarém, and when ISA was around 0.2 in Lucas for the per-pixel based results. For the fraction-based method, ISA was still overestimated for the majority of the sectors in Santarém, but in Lucas, when ISA in a sector was less than 0.2, ISA was mainly overestimated, but after ISA in a sector was greater than 0.6, ISA was underestimated.

Analysis of the RMSE results at fractional and per-pixel scales for both study areas indicated that per-pixel based results had much higher estimation errors for each ISA category than fraction-based results, except when ISA was in the very high category in Lucas (see Table 1). For both study areas, the estimate errors for per-pixel based results had the highest errors when ISA in a sector fell in the low and medium categories, and had

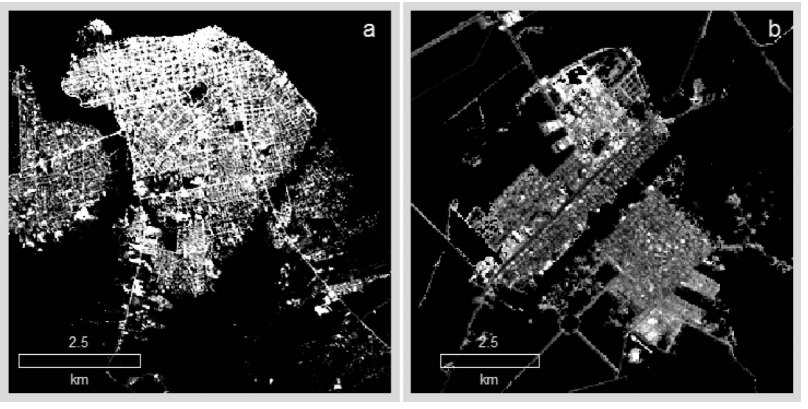

Figure 6. Impervious surface images in Santarém (a) and Lucas (b), which were developed from Landsat TM images using the fraction-based method.

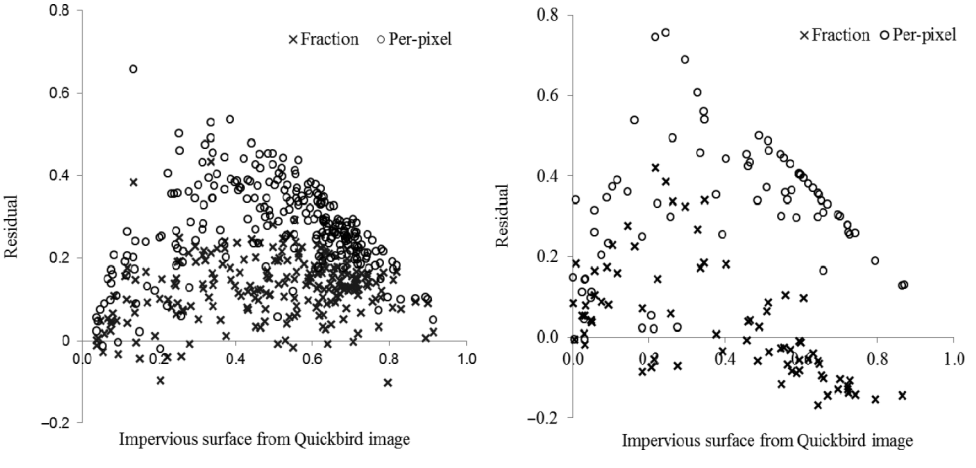

Figure 7. Comparison of residual distribution between fraction-based and per-pixel based methods for Santarém (Left) and Lucas (Right) study areas.

Table 1. Assessment of impervious surface estimation results from Landsat TM images for both study areas.

		Santarém			Lucas		
Category of ISA	Data ranges	Fraction	Per-pixel	#	Fraction	Per-pixel	#
Very low	<0.2	0.108	0.193	27	0.130	0.255	21
Low	0.2–0.4	0.163	0.343	44	0.236	0.477	15
Medium	0.4–0.6	0.161	0.351	67	0.072	0.409	21
High	0.6–0.8	0.147	0.259	95	0.122	0.307	18
Very high	>0.8	0.100	0.134	8	0.186	0.128	2
Total		0.149	0.295	241	0.146	0.361	77

Note: # represents number of census sectors at each ISA category.

lowest errors when ISA fell in the very high category. As the proportion of ISA in a census sector increased, from low to very high, the RMSE in per-pixel based results decreased in both study areas. For fraction-based results, the RMSE gradually decreased from the low to very high category in Santarém, but the RMSE in Lucas was lowest when ISA was in the medium category, and had relatively high RMSE when ISA was in the very high category. Figure 7 indicates that when ISA fell within 0.4–0.6 in Lucas, the residuals had positive and negative values, thus, the overall estimate had high accuracy in this category. When fraction values were greater than 0.6, residuals became negative, implying that ISA was underestimated.

The RMSE at per-pixel level was higher in Lucas than in Santarém, maybe due to the relatively smaller urban extent and lower ISA proportion in a unit in Lucas, as shown in Figure 5. This highlights the potential for problems in using the per-pixel based method for ISA estimation when the study area has a small urban extent or is in an urban–rural landscape. In the fractional ISA results, ISA estimates had the highest estimation error at the low category for both study areas, implying the difficulty in accurately extracting ISA in urban–rural or rural landscape due to the confusion of ISA and bare soils, and the dominance of non-ISA land covers within a pixel. The lowest RMSE in Santarém and relatively high RMSE in Lucas when ISA was in very high category imply the different impacts of urban patterns on ISA estimation.

The overestimation of ISA in Santarém may be due to (1) the underestimation of reference data from the 2008 QuickBird image, because it was acquired 2 years before the 2010 TM image, (2) the spectral confusion of dark ISA with shadows and water resulted in overestimation of dark ISA and (3) the spectral confusion of some bright ISA and bare soils during the dry season resulted in the overestimation of some bright ISA, especially in suburban areas. For per-pixel based results, a large proportion of the overestimation is due to the mixture of ISA and other land covers within a pixel. In Lucas, when ISA accounts for greater than 0.6 in a census sector, ISA is underestimated when the fraction-based method is used. This is mainly due to the difficulty in effectively extracting ISA under tree cover and shadow areas cast by trees and tall buildings. As shown in Figure 3f, very

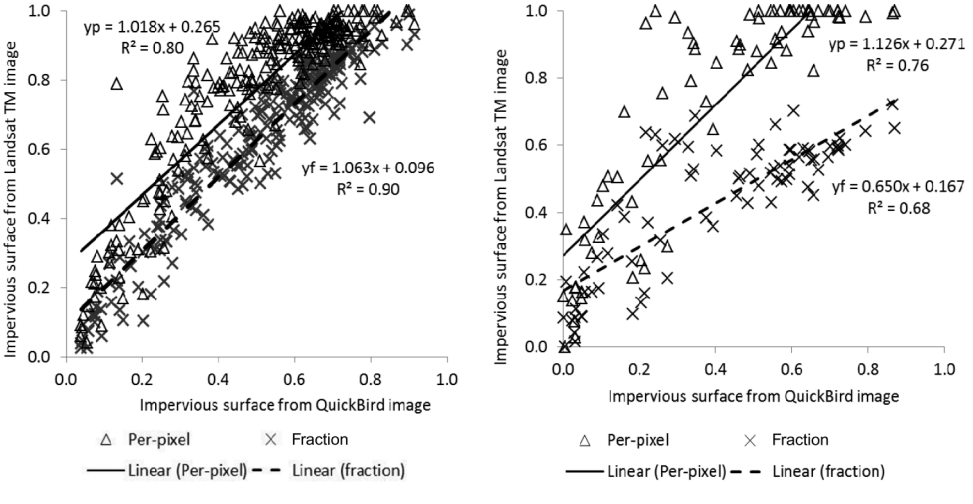

Figure 8. Relationship between estimates from Landsat TM image and reference data from QuickBird images for Santarém (Left) and Lucas (Right).

limited ISA was extracted in the low-albedo fraction image in Lucas, as compared to Figure 3b for Santarém. The situation of overestimation when ISA was in low value and of underestimation when ISA was in high value is similar to previous research (Wu and Murray 2003; Lu and Weng 2006; Lu, Moran, and Hetrick 2011).

The above analysis indicates the overestimation of ISA, especially in per-pixel based results. However, the relationship between estimate and reference shown in Figure 8 indicates that there is a good linear relationship between the estimate and reference data in both per-pixel based and fraction-based methods. Therefore, the estimates can be improved by establishing a linear regression model through integrating the ISA estimates and reference data from a high spatial resolution image. Our previous research has confirmed the importance of implementing the calibration of Landsat-derived ISA estimates for improving ISA estimation performance (Lu, Moran, and Hetrick 2011). In particular, this kind of calibration is necessary when the study area contains a large proportion of urban–rural landscape and accurate area statistics are required. Because different sources of remote sensing data are available, integrated use of multi-sensor and multi-spatial resolution images have been used to improve ISA mapping performance (Yang et al. 2009; Tullis et al. 2010; Lu, Li, et al., 2011).

5. Conclusions

This research identified the challenges of ISA estimation using Landsat TM images in urban–rural frontiers. The per-pixel based method considerably overestimated the ISA results and the fraction-based method considerably reduced this problem. Overall, fraction-based results had RMSE of 0.15 for both study areas, and per-pixel based results had RMSE as high as 0.30 in Santarém and 0.36 in Lucas. When emphasis is on area statistical results, the fraction-based ISA mapping method is recommended. If reference data are available, calibration of the estimates from Landsat TM images is necessary, especially when the study areas cover urban–rural landscapes. This research proposes a promising method for mapping fractional ISA distribution in the complex urban–rural landscape in the Brazilian Amazon, and can be easily transferred to other study areas. More research is needed to calibrate the ISA estimation through integration of very high spatial resolution images.

Acknowledgements

The authors wish to thank the National Institute of Child Health and Human Development at NIH (Grant No. R01 HD035811) for the support of this research, addressing population and environment reciprocal interactions in several regions of the Brazilian Amazon. Any errors are solely the responsibility of the authors and not of the funding agencies.

References

Arnold, C. L., and C. J. Gibbons. 1996. “Imperious Surface Coverage: The Emergence of a Key Environmental Indicator.” *Journal of the American Planning Association* 62 (2): 243–258.

Brabec, E., S. Schulte, and P. L. Richards. 2002. “Impervious Surface and Water Quality: A Review of Current Literature and Its Implications for Watershed Planning.” *Journal of Planning Literature* 16 (4): 499–514.

Chander, G., B. L. Markham, and D. L. Helder. 2009. “Summary of Current Radiometric Calibration Coefficients for Landsat MSS, TM, ETM +, and EO-1 ALI Sensors.” *Remote Sensing of Environment* 113: 893–903.

Chavez, P. S. Jr. 1996. "Image-Based Atmospheric Corrections – Revisited and Improved." *Photogrammetric Engineering and Remote Sensing* 62: 1025–1036.
Goetz, S. J., R. Wright, A. J. Smith, E. Zinecker, and E. Schaub. 2003. "Ikonos Imagery for Resource Management: Tree Cover, Impervious Surface, and Riparian Buffer Analyses in the Mid-Atlantic Region." *Remote Sensing of Environment* 88: 195–208.
Lu, D., S. Hetrick, and E. Moran. 2011. "Impervious Surface Mapping with QuickBird Imagery." *International Journal of Remote Sensing* 32 (9): 2519–2533.
Lu, D., G. Li, E. Moran, M. Batistella, and C. Freitas. 2011. "Mapping Impervious Surfaces with the Integrated Use of Landsat Thematic Mapper and Radar Data: A Case Study in an Urban-Rural Landscape in the Brazilian Amazon." *ISPRS Journal of Photogrammetry and Remote Sensing* 66 (6): 798–808.
Lu, D., E. Moran, and S. Hetrick. 2011. "Detection of Impervious Surface Change with Multitemporal Landsat Images in an Urban-Rural Frontier." *ISPRS Journal of Photogrammetry and Remote Sensing* 66 (3): 298–306.
Lu, D., E. Moran, S. Hetrick, and G. Li. 2012, "Mapping Impervious Surface Distribution with the Integration of Landsat TM and QuickBird Images in a Complex Urban-Rural Frontier in Brazil (Chapter 13)." In *Environmental Remote Sensing and Systems Analysis,* edited by Ni.-B. Chang, 277–296. Boca Raton, FL: CRC Press/Taylor and Francis.
Lu, D., and Q. Weng. 2004. "Spectral Mixture Analysis of the Urban Landscapes in Indianapolis with Landsat ETM+ Imagery." *Photogrammetric Engineering and Remote Sensing* 70: 1053–1062.
Lu, D., and Q. Weng. 2006. "Use of Impervious Surface in Urban Land Use Classification." *Remote Sensing of Environment* 102: 146–160.
Lu, D., X. Xu, H. Tian, E. Moran, M. Zhao, and S. Running. 2010. "The Effects of Urbanization on Net Primary Productivity in Southeastern China." *Environmental Management* 46 (3): 404–410.
Myint, S. W., A. Brazel, G. Okin, and A. Buyantuyev. 2010. "Combined Effects of Impervious Surface and Vegetation Cover on Air Temperature Variations in a Rapidly Expanding Desert City." *GIScience & Remote Sensing* 47 (3): 301–320.
Ridd, M. K. 1995. "Exploring a V-I-S (Vegetation-Impervious Surface-Soil) Model for Urban Ecosystem Analysis Through Remote Sensing: Comparative Anatomy for Cities." *International Journal of Remote Sensing* 16 (12): 2165–2185.
Schueler, T. R. 1994. "The Importance of Imperviousness." *Watershed Protection Techniques* 1: 100–111.
Slonecker, E. T., D. Jennings, and D. Garofalo. 2001. "Remote Sensing of Impervious Surface: A Review." *Remote Sensing Reviews* 20 (3): 227–255.
Slonecker, E. T., and J. S. Tilley. 2004. "An Evaluation of the Individual Components and Accuracies Associated with the Determination of Impervious Area." *GIScience & Remote Sensing* 41 (2): 165–184.
Tullis, J. A., J. R. Jensen, G. T. Raber, and A. M. Filippi. 2010. "Spatial Scale Management Experiments Using Optical Aerial Imagery and LIDAR Data Synergy." *GIScience & Remote Sensing* 47 (3): 338–359.
Weng, Q. ed. 2007. *Remote Sensing of Impervious Surfaces*. Boca Raton, FL: Taylor & Francis Group, LLC.
Weng, Q. 2012. "Remote Sensing of Impervious Surfaces in the Urban Areas: Requirements, Methods, and Trends." *Remote Sensing of Environment* 117 (2): 34–49.
Wu, C. 2004. "Normalized Spectral Mixture Analysis for Monitoring Urban Composition Using ETM+ Imagery." *Remote Sensing of Environment* 93: 480–492.
Wu, C., and A. T. Murray. 2003. "Estimating Impervious Surface Distribution by Spectral Mixture Analysis." *Remote Sensing of Environment* 84: 493–505.
Yang, L., L. Jiang, H. Lin, and M. Liao. 2009. "Quantifying Sub-Pixel Urban Impervious Surface Through Fusion of Optical and InSAR Imagery." *GIScience & Remote Sensing* 46 (2): 161–171.
Zug, M., L. Phan, D. Bellefleur, and O. Scrivener. 1999. "Pollution Wash-Off Modeling on Impervious Surface: Calibration, Validation, and Transposition." *Water Science and Technology* 39: 17–24.